

# Transport of particles for a spatially periodic stochastic system with correlated noises

 Jing-hui Li,<sup>1</sup> Jerzy Łuczka,<sup>1,2</sup> and Peter Hänggi<sup>1</sup>
<sup>1</sup>*Lehrstuhl für Theoretische Physik I, Institut für Physik, Universität Augsburg, Universitätsstrasse 1, D-86135 Augsburg, Germany*
<sup>2</sup>*Institute of Physics, Silesian University, 40-007 Katowice, Poland*

(Received 25 October 2000; published 26 June 2001)

The transport of particles for a spatially periodic stochastic system driven by two multiplicative noises and one additive noise (between which there are correlations) is investigated for the overdamped and underdamped cases. It is shown that (i) the probability current can be positive, zero, or negative; (ii) the movement of the particles represents the phenomenon of resonance as a function of the additive noise strength. For the underdamped case, the particles with different mass can be separated by controlling the system or the noise parameters. In particular, a reversal of the flux can be induced by controlling the correlations between the additive and multiplicative noises.

DOI: 10.1103/PhysRevE.64.011113

PACS number(s): 05.40.Ca, 82.40.Bj, 87.10.+e

## I. INTRODUCTION

Recently, there has been increasing interest in studying the noise-induced transport of Brownian particles for systems with a spatially periodic potential field. It has been shown that the asymmetry of the potential [1,2], the asymmetry of the driving noise [3], and the input signal (no noise, time correlation, or constant) [1,4] are ingredients for the transport.

The recent burst of this work is motivated in part by the challenge of explaining the unidirectional transport of molecular motors in the biological realm [5]. Another source of motivation arises from the new methods of separation or segregation of Brownian particles [6], and more recently in the recognition of the ‘‘ratchet effect’’ [1,7]. Now the idea of noise-caused transport has been applied to biomolecular motor systems, Brownian motor systems, and quantum systems [including surface electromigration, Josephson-junction arrays, cold atoms (with an asymmetric optical lattice), superconductors, and semiconductor heterstructures (with rocked electron ratchets)].

However, most of the models (classical, not quantum) so far deal with overdamped Brownian particles in which the inertial term due to the finite mass of the particles is neglected. The transport of underdamped particles in systems driven by noise has been studied only in a few works [8] that consider the mass of the particle. In this paper, we shall consider a model with a spatially periodic potential driven by one additive noise and two multiplicative noises, which are correlated, and investigate the transport of particles in the overdamped and underdamped cases.

## II. MODEL

We consider a model whose Langevin equation is (in dimensionless form)

$$m\ddot{x} + \dot{x} = f(x) - \xi_1(t)g_1(x) - \xi_2(t)g_2(x) + \eta(t), \quad (1)$$

where  $f(x) = -J_1 \sin(x/2) - J_2 \sin(x+x_0)$ ,  $g_1(x) = \sin(x/2)$ , and  $g_2(x) = \sin(x+x_0)$ . [The common period of the functions  $f(x)$ ,  $g_1(x)$ , and  $g_2(x)$  is  $4\pi$ .] The multiplicative noises  $\xi_i(t)$  ( $i=1,2$ ) and the additive noise  $\eta(t)$  represent Gaussian white noises, and  $m$  is the value of dimensionless mass for

the particle. (Here the viscous friction strength is assumed to equal 1.) In general, we express the influence of internal fluctuations on the system as additive noise and the effect of external environmental fluctuations on the system as multiplicative noise. Here we assume that the external environmental fluctuations can influence the internal fluctuations. So the additive and multiplicative noises are not independent (there are correlations between them). The statistical properties of  $\xi_i(t)$  ( $i=1,2$ ) and  $\eta(t)$  are  $\langle \xi_i(t) \rangle_f = \langle \eta(t) \rangle_f = 0$ ,  $\langle \xi_i(t) \xi_j(t') \rangle_f = 2D_i \delta_{ij} \delta(t-t')$ ,  $\langle \eta(t) \eta(t') \rangle_f = 2D \delta(t-t')$ , and  $\langle \eta(t) \xi_i(t') \rangle_f = 2\lambda_i \sqrt{DD_i} \delta(t-t')$  ( $-1 \leq \lambda_i \leq 1$ ), where  $\langle \rangle_f$  represents the average over noise. In this paper, Eq. (1) is given in dimensionless form, so the variables  $x$  and  $t$  and the parameters  $D$ ,  $D_i$ ,  $\lambda_i$ , and  $m$  are dimensionless.

Equation (1) can be transformed into

$$m\ddot{x} + \dot{x} = f(x) + \xi_1(t)[- \sin(x/2) + \lambda_1 \sqrt{D/D_1}] + \xi_2(t)[- \sin(x+x_0) + \lambda_2 \sqrt{D/D_2}] + \eta'(t), \quad (2)$$

in which  $\eta'(t) = \eta(t) - \lambda_1 \sqrt{D/D_1} \xi_1(t) - \lambda_2 \sqrt{D/D_2} \xi_2(t)$ . The statistical properties of  $\eta'(t)$  are  $\langle \eta'(t) \rangle = 0$  and  $\langle \eta'(t) \eta'(t') \rangle = 2D(1 - \lambda_1^2 - \lambda_2^2) \delta(t-t')$ . Here the noises  $\xi_i(t)$  and  $\eta'(t)$  are no longer correlated.

## III. OVERDAMPED CASE

For the overdamped case, one can use the adiabatic approximation  $\ddot{x} = 0$ . Then Eq. (2) becomes

$$\dot{x} = f(x) + \xi_1(t)[- \sin(x/2) + \lambda_1 \sqrt{D/D_1}] + \xi_2(t)[- \sin(x+x_0) + \lambda_2 \sqrt{D/D_2}] + \eta'(t). \quad (3)$$

The Stratonovich interpretation of the stochastic differential equation (3) yields the Fokker-Planck equation [9]

$$\partial_t P(x,t) = -\partial_x A(x)P(x,t) + \partial_x^2 B(x)P(x,t), \quad (4)$$

where  $A(x) = -J_1 \sin(x/2) - J_2 \sin(x+x_0) + (D_1/4) \sin x + (D_2/2) \sin[2(x+x_0)] - (\lambda_1 \sqrt{DD_1}/2) \cos(x/2) - (\lambda_2 \sqrt{DD_2}) \cos(x+x_0)$ , and  $B(x) = D_1 \sin^2(x/2) + D_2 \sin^2(x+x_0) + D - 2\lambda_1 \sqrt{DD_1} \times \sin(x/2) - 2\lambda_2 \sqrt{DD_2} \sin(x+x_0)$ . The periodic boundary condition for Eq. (4) is  $P(a,t) = P(a+4\pi,t)$  (here we take  $a=0$ ).

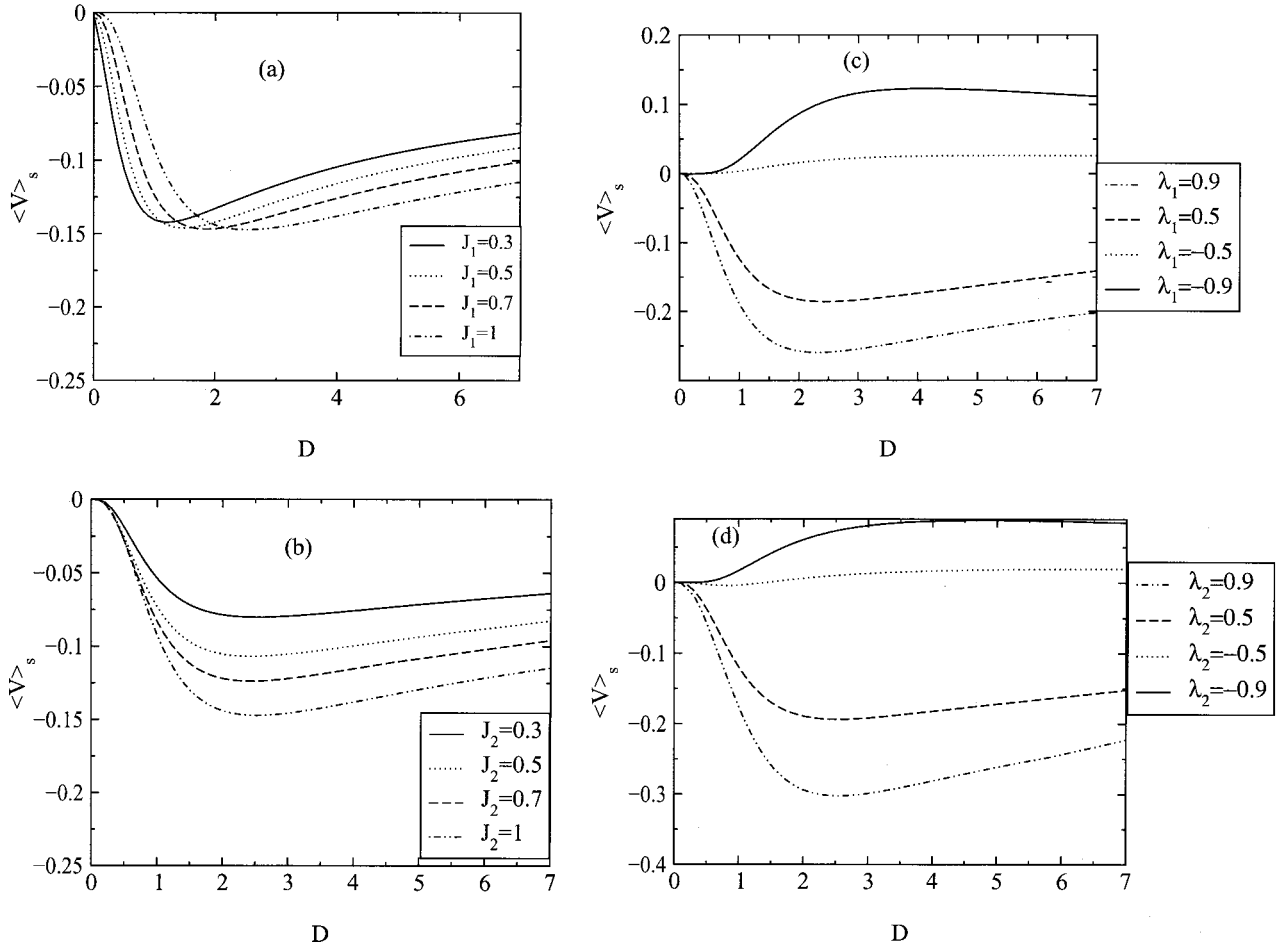


FIG. 1. The average velocity versus the additive noise strength in the overdamped case for the model (1). (a) corresponds to the average velocity versus the additive noise strength for different values of  $J_1$  ( $J_1=0.3, 0.5, 0.7$  and  $1$ , respectively) with  $J_2=1, x_0=\pi/2, D_1=D_2=0.3$ , and  $\lambda_1=\lambda_2=0.3$ ; (b) to that for different values of  $J_2$  ( $J_2=0.3, 0.5, 0.7$  and  $1$ , respectively) with  $J_1=1, x_0=\pi/2, D_1=D_2=0.3$ , and  $\lambda_1=\lambda_2=0.3$ ; (c) to that for different values of  $\lambda_1$  ( $\lambda_1=0.9, 0.5, -0.5$ , and  $-0.9$ , respectively) with  $J_1=J_2=1, x_0=\pi/2$ , and  $D_1=D_2=0.3$ , and  $\lambda_2=0.3$ ; (d) to that for different values of  $\lambda_2$  ( $\lambda_2=0.9, 0.5, -0.5$ , and  $-0.9$ , respectively) with  $J_1=J_2=1, x_0=\pi/2, D_1=D_2=0.3$ , and  $\lambda_1=0.3$ .

The average velocity is given by

$$\langle V(t) \rangle = \langle \langle V(x, t) \rangle_x \rangle_f = \langle \langle \dot{x} \rangle_x \rangle_f, \quad (5)$$

where  $\langle \rangle_x$  stands for the average over  $x$ .

Under periodic boundary conditions, the stationary solution of Eq. (4) is [9]

$$P_s(x) = N \frac{e^{\Phi(x)}}{B(x)} \int_0^{4\pi} dx' e^{-\Phi(x') - \Phi(4\pi)\theta(x-x')}. \quad (6)$$

Here  $\Phi(x) = \int_0^x [A(x')/B(x')] dx'$ ,  $\theta(x-x')$  is the Heaviside step function, and  $N$  a normalized constant.

From Eqs. (5) and (6), we obtain

$$\begin{aligned} \langle V \rangle_s &= \langle \dot{x} \rangle_s \\ &= \lim_{t \rightarrow \infty} \frac{1}{t} \int_0^t \langle \langle V(x, \tau) \rangle_x \rangle_f d\tau \\ &= \langle A(x) \rangle_s \end{aligned}$$

$$\begin{aligned} &= N \int_0^{4\pi} dx \frac{A(x) e^{\Phi(x)}}{B(x)} \int_0^{4\pi} dx' e^{-\Phi(x') - \Phi(4\pi)\theta(x-x')} \\ &= 4\pi N [1 - e^{-\Phi(4\pi)}]. \end{aligned} \quad (7)$$

The probability current  $J$  can be obtained from  $\partial_x J = -\partial_x A P + \partial_x^2 B P$ , i.e.,  $J = -AP + \partial_x B P$ . It is easy to obtain

$$J = N [1 - e^{-\Phi(4\pi)}] = \langle V \rangle_s / (4\pi). \quad (8)$$

Equations (7) and (8) show that the condition under which the flux changes sign is that the value  $\Phi(4\pi)$  can vary from positive to negative or vice versa.

In Fig. 1 we plot the average velocity versus the additive noise strength  $D$  from Eq. (7). The Fig. 1(a) corresponds to the average velocity versus the additive noise strength for different values of  $J_1$  ( $J_1=0.3, 0.5, 0.7$  and  $1$ , respectively) with  $J_2=1, D_1=D_2=0.3$ , and  $\lambda_1=\lambda_2=0.3$ ; Fig. 1(b) to that for different values of  $J_2$  ( $J_2=0.3, 0.5, 0.7$ , and  $1$ , respectively) with  $J_1=1, D_1=D_2=0.3$ , and  $\lambda_1=\lambda_2=0.3$ ; the

Fig. 1(c) to that for different values of  $\lambda_1$  ( $\lambda_1=0.9, 0.5, -0.5,$  and  $-0.9,$  respectively) with  $J_1=J_2=1, D_1=D_2=0.3,$  and  $\lambda_2=0.3$ ; and Fig. 1(d) to that for different values of  $\lambda_2$  ( $\lambda_2=0.9, 0.5, -0.5,$  and  $-0.9,$  respectively) with  $J_1=J_2=1, D_1=D_2=0.3,$  and  $\lambda_1=0.3$ . The figures show that (a) the absolute value of the average velocity is a nonmonotonic function of the additive noise strength and has a clear peak value, which is a manifestation of the phenomenon of resonance; and (b) the average velocity may be negative, zero, or positive.

Here we wish to give some explanation for the origin of the average velocity. First, when  $\xi_i(t)=0$  ( $i=1,2$ ) no average velocity can be produced. A nonzero average velocity with  $\xi_i(t)=0$  means that only thermal fluctuation is converted into work and implies a violation of the second law of thermodynamics. Second, if  $\lambda_1=\lambda_2=0$  and the function  $f(x)$  is symmetric, no average velocity can be caused, since no symmetry breaking happens. So the multiplicative noises, the correlations between the additive and multiplicative noises, and the asymmetry of  $f(x)$  [or the asymmetry of the potential, which is  $U(x)=-\int^x f(x')dx'$ ] are ingredients for the average velocity for the model (1). The reason for producing the average velocity is that the symmetry of the system is broken by the function  $f(x)$ , or the correlations between the additive and multiplicative noises. Now the asymmetry of the system makes the probability of fluctuations on the two sides of the potential barrier different, so that an average velocity arises. The energy in response to the average velocity stems from the noise.

The phenomenon of resonance happening here is analyzed below. In Figs. 1(a)–1(d), the additive noise plays a twofold role. On one hand, it stimulates directional motion of the particle in response to the asymmetric condition of the system. On the other hand, it reduces the asymmetry of the system, which is the cause of directional motion of the particle. The competition of these two apparently opposite roles produces a peak at which a phenomenon of resonance appears.

The characteristics of the constant force  $I$  versus the average velocity can be calculated from Eq. (7) if  $A(x)+I$  is used to replace  $A(x)$  (including  $A(x')$  in  $\Phi(x)=\int_0^x[A(x')/B(x')]dx'$ ). In Figs. 2(a) and 2(b) we plot the characteristics of the average velocity versus the constant force for different values of the additive noise strength. Figure 2(a) corresponds to  $D=0.2, 0.5, 0.7,$  and  $1,$  and Fig. 2(b) to  $D=1, 2, 3,$  and  $4$  [in Fig. 2(b), the diagonal line is without noise]. From these figures, we find the following. (a) With increase of the additive noise strength, the curve for the average velocity versus the value of the constant force is nearer and nearer to the one without noise. This is because of the cooperative action of the multiplicative noises, the correlations between the additive and multiplicative noises, and the asymmetry of the potential. (b) One can manipulate the behavior of the average velocity versus the constant force by controlling the additive noise strength. Now one can appropriately adjust the temperature to make the average velocity versus the constant force fit one's demands (since the thermal additive noise strength  $D$  is proportional to the temperature). In addition, further study shows that when the constant

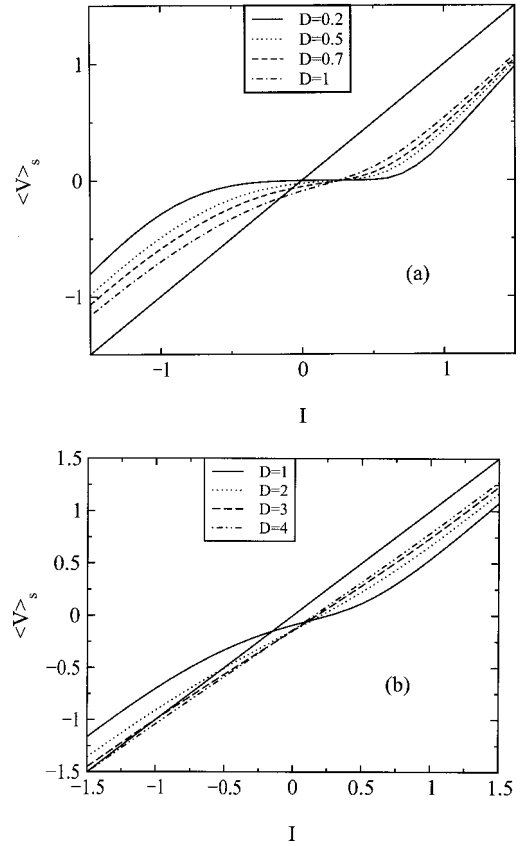


FIG. 2. The average velocity versus the constant force in the overdamped case for the model (1). (a) corresponds to  $D=0.2, 0.5, 0.7,$  and  $1,$  and (b) to  $D=1, 2, 3,$  and  $4$  (the diagonal line is the case without noise), with  $D_1=D_2=0.3, x_0=\pi/2, \lambda_1=\lambda_2=0.3,$  and  $J_1=J_2=1$ .

force is not zero the average velocity versus the additive noise strength presents the same phenomena of resonance as in Figs. 1(a)–1(d).

#### IV. UNDERDAMPED CASE

In this section we shall consider the transport of particles in the case of  $m \neq 0$ . For the convenience of analysis and calculation, we write Eq. (1) as

$$\dot{x} = y,$$

$$\dot{y} = -\frac{1}{m}y + f'(x) + g_1(x)\xi_1(t) + g_2(x)\xi_2(t) + \frac{1}{m}\eta'(t), \quad (9)$$

where  $f'(x) = -(1/m)[J_1 \sin(x/2) + J_2 \sin(x+x_0)],$   $g_1(x) = (1/m)[- \sin(x/2) + \lambda_1 \sqrt{D/D_1}],$  and  $g_2(x) = (1/m)[- \sin(x+x_0) + \lambda_2 \sqrt{D/D_2}].$  In the Stratonovich case, the Fokker-Planck equation for the probability density  $P(x,y,t)$  corresponding to Eq. (9) is

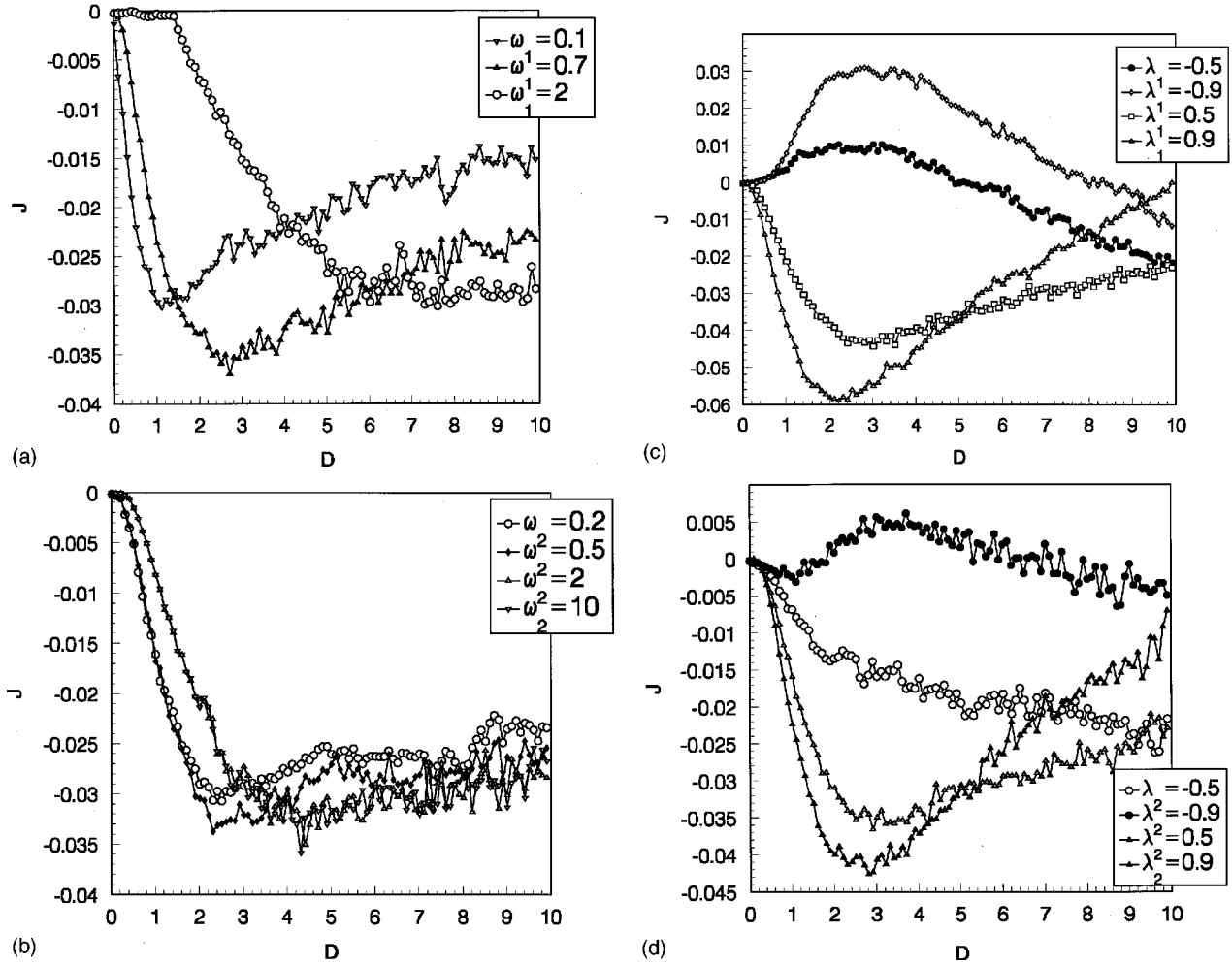


FIG. 3. The current  $J$  versus the additive noise strength in the underdamped case for the model (1). (a) is for different values of  $J_1$  ( $J_1=0.1, 0.7$ , and  $2$ , respectively) with  $D_1=D_2=0.3$ ,  $J_2=1$ ,  $x_0=\pi/2$ ,  $\lambda_1=\lambda_2=0.3$ , and  $m=5$ ; (b) is for different values of  $J_2$  ( $J_2=0.2, 0.5$ ,  $2$  and  $10$ , respectively) with  $D_1=D_2=0.3$ ,  $J_1=1$ ,  $x_0=\pi/2$ ,  $\lambda_1=\lambda_2=0.3$ , and  $m=5$ ; (c) is for different values of  $\lambda_1$  ( $\lambda_1=-0.9, -0.5, 0.5$ , and  $0.9$ , respectively) with  $D_1=D_2=0.3$ ,  $x_0=\pi/2$ ,  $J_1=J_2=1$ ,  $\lambda_2=0.3$ , and  $m=5$ ; (d) is for different values of  $\lambda_2$  ( $\lambda_2=-0.9, -0.5, 0.5$ , and  $0.9$ , respectively) with  $D_1=D_2=0.3$ ,  $x_0=\pi/2$ ,  $J_1=J_2=1$ ,  $\lambda_1=0.3$ , and  $m=5$ .

$$\begin{aligned} \partial_t P = & -y \partial_x P - \partial_y \left[ -\frac{1}{m} y + f'(x) \right] P \\ & + \left\{ \frac{1}{m} D (1 - \lambda_1^2 - \lambda_2^2) + D_1 [g_1(x)]^2 \right. \\ & \left. + D_2 [g_2(x)]^2 \right\} \partial_y^2 P. \end{aligned} \quad (10)$$

Equation (10) cannot be solved analytically even for the stationary case since detailed balance is broken and the probability flow is not zero, but it can be solved by applying numerical methods. In the following we carry out our numerical simulation directly using the Langevin equation (9). From Ref. [10] we can get the numerical algorithm

$$\begin{aligned} x(t+\Delta t) &= x(t) + y \Delta t, \\ y(t+\Delta t) &= y(t) + \left( -\frac{1}{m} y(t) + f'(x(t)) \right) \Delta t \\ &+ x_1(t, \Delta t) + x_2(t, \Delta t), \end{aligned} \quad (11)$$

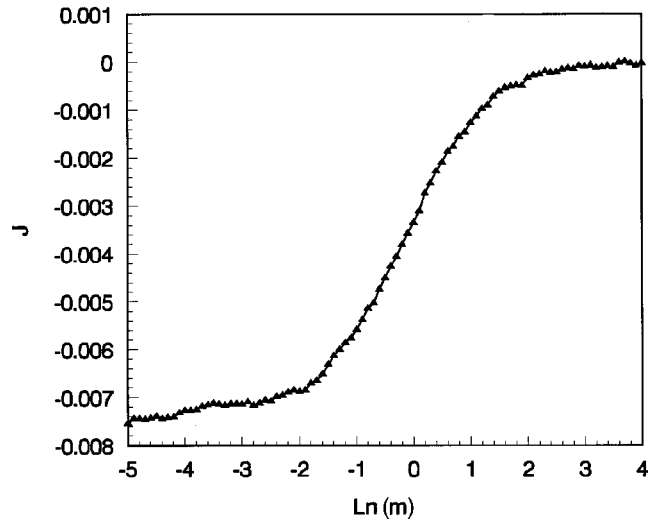


FIG. 4. The current  $J$  as a function of the natural logarithm of the mass with  $D_1=D_2=0.3$ ,  $J_1=J_2=1$ ,  $x_0=\pi/2$ ,  $\lambda_1=\lambda_2=0.3$ , and  $D=0.3$ .

where

$$\begin{aligned}
 x_1(t, \Delta t) = & \left\{ D_1 g_1(x(t)) \frac{\partial g_1(x(t))}{\partial x} \phi_1^2 \right. \\
 & + D_2 g_2(x(t)) \frac{\partial g_2(x(t))}{\partial x} \phi_1^2 \\
 & + \sqrt{D_1 D_2} \left[ g_1(x(t)) \frac{\partial g_2(x(t))}{\partial x} \right. \\
 & \left. + g_2(x(t)) \frac{\partial g_1(x(t))}{\partial x} \right] \phi_1 \phi_2 \\
 & + \sqrt{D D_1 / m} \frac{\partial}{\partial x} g_1(x(t)) \phi \phi_1 \\
 & \left. + \sqrt{D D_2 / m} \frac{\partial}{\partial x} g_1(x(t)) \phi \phi_2 \right\} \Delta t,
 \end{aligned}$$

and

$$\begin{aligned}
 x_2(t, \Delta t) = & g_1(x(t)) \sqrt{2 D_1 \Delta t} \phi_1 + g_2(x(t)) \sqrt{2 D_2 \Delta t} \phi_2 \\
 & + \sqrt{2 D \Delta t / m} \phi,
 \end{aligned}$$

with three independent Gaussian random numbers  $\phi_1$ ,  $\phi_2$ , and  $\phi$  of zero mean and variance 1. Here we define the current  $J$  which is averaged over an ensemble of initial conditions for the average velocity. Therefore, the current has two different averages. The first average is over  $M$  initial conditions, which we take equally distributed in space (from  $x=0$  to  $x=4\pi$ ), and with a zero initial velocity. For a fixed time  $t_j$ , we can obtain the first average  $v_j = (1/M) \sum_{i=1}^M \dot{x}_i(t_j)$ . The second average is a time average. Since we take a discrete time for the numerical simulation, we have a discrete finite set of  $N$  different times  $t_j$ . Then the current is defined as  $J = (1/N) \sum_{j=1}^N v_j$ .

The numerical results are plotted in Figs. 3(a)–3(d) for the current versus the additive noise strength. Every point in the figures is calculated by taking the average of the

$M=400$  initial conditions and the  $N=10^5$  different discrete times (averaged by  $4 \times 10^7$  points). Here the time step is taken as  $\Delta t=0.01$ . In order to guarantee that the system is in the stationary state, we take the time average after  $t=1000$ . This average is taken from  $t=1000$  to  $t=2000$ . The space from  $x=0$  to  $x=4\pi$  is divided into 400 ( $x_i = 4\pi i/400$ ,  $i=1, 2, \dots, 400$ ). The initial conditions are  $x_i(t=0)=0$  ( $i=1, 2, 3, \dots, 400$ ). From the figures we can see that (a) the current can be negative, zero, or positive; (b) for the transport there are the phenomena of resonance. It is interesting that Figs. 3(a)–3(d) and Figs. 1(a)–1(d) (overdamped case) have the same characteristics (a) and (b). In addition, they have other similar features [these are less important than the above (a) and (b)]. (1) With the increase of  $J_1$  or  $J_2$ , the peaks move to the right. (2) With increase in the absolute value of  $\lambda_1$  or  $\lambda_2$ , the transport can be strengthened. It is also interesting that by varying the value of  $\lambda_1$  or  $\lambda_2$  the flux can be reversed, that can be observed in Figs. 3(c) and 3(d). If the additive noise strength is large enough, a reversal can also be induced [cf. Fig. 3(c)]. The phenomenon of transport and its resonance happening here have the same origins as the ones analyzed in the overdamped case.

Finally, let us consider the transport of particles with different mass. The result of a simulation for the current  $J$  versus the natural logarithm of the mass is depicted in Fig. 4 with the parameters  $D_1=D_2=0.3$ ,  $J_1=J_2=1$ ,  $x_0=\pi/2$ ,  $\lambda_1=\lambda_2=0.3$ , and  $D=0.3$ . From Fig. 4 we see that with decreasing mass of the particle, the particle moves more and more quickly. Thus we can separate the particles with different values of mass by controlling the parameters of the noise (i.e.,  $D$ ,  $D_1$ ,  $D_2$ ,  $\lambda_1$ , and  $\lambda_2$ ) or the parameters of the potential (i.e.,  $J_1$ ,  $J_2$ , and  $x_0$ ). For the parameters given in Fig. 4, the particles with small inertia move to the negative direction quickly, while the particles with strong inertia move slowly or almost remain in the original position.

#### ACKNOWLEDGMENTS

This research was supported by the Alexander von Humboldt Foundation, and also by KBN (Poland), Grant No. 2 P03B 160 17.

- [1] M. O. Magnasco, Phys. Rev. Lett. **71**, 1477 (1993).  
 [2] R. Bartussek, P. Hänggi, and J. G. Kissner, Europhys. Lett. **28**, 459 (1994); M. M. Millonas and M. I. Dykman, Phys. Lett. A **185**, 65 (1994); C. Doering, W. Hortheke, and J. Riordan, *ibid.* **72**, 2984 (1994); J.-F. Chauwin, L. Peliti, and A. Ajdari, Phys. Rev. Lett. **72**, 2652 (1994); R. D. Astumian and M. Bier, *ibid.* **72**, 1766 (1994); M. Bier, Phys. Lett. A **211**, 12 (1996); M. Bier and R. D. Astumian, Phys. Rev. Lett. **76**, 4277 (1996); P. Reimann, R. Bartussek, R. Häußler, and P. Hänggi, Phys. Lett. A **215**, 26 (1996); H. Kamegawa, T. Hondou, and F. Takagi, Phys. Rev. Lett. **80**, 5251 (1998); B. Lindner, L. Schimansky-Geier, P. Reimann, P. Hänggi, and M. Nagaoka, Phys. Rev. E **59**, 1417 (1999); A. Sarmiento and H. Larralde, *ibid.* **59**, 4878 (1999).  
 [3] J. Łuczka, R. Bartussek, and P. Hänggi, Europhys. Lett. **31**,

- 431 (1995); D. R. Chialvo, and M. M. Millonas, Phys. Lett. A **209**, 26 (1995); A. Ajdari, D. Mukamel, L. Peliti, and J. Prost, J. Phys. I **14**, 1551 (1994); M. C. Mahato and A. M. Jayannavar, Phys. Lett. A **209**, 21 (1995); M. M. Millonas and D. R. Chialvo, Phys. Rev. E **53**, 2239 (1996); P. Jung, J. G. Kissner, and P. Hänggi, Phys. Rev. Lett. **76**, 3436 (1996); I. Zapata, J. Łuczka, F. Sols, and P. Hänggi, *ibid.* **80**, 829 (1998); J. H. Li and Z. Q. Huang, Phys. Rev. E **58**, 139 (1998).  
 [4] I. Zapata, R. Bartussek, F. Sols, and P. Hänggi, Phys. Rev. Lett. **77**, 2292 (1996); J. H. Li and Z. Q. Huang, Phys. Rev. E **57**, 3917 (1998).  
 [5] C. Peskin, G. B. Ermentrout, and G. Oster, in *Cell Mechanics and Cellular Engineering*, edited by V. Mow *et al.* (Springer, Berlin, 1994).  
 [6] J. Rousselet, L. Salome, A. Ajdari, and J. Prost, Nature (London) **370**, 446 (1994).

- [7] J. F. Chauwin, A. Ajdari, and J. Prost, *Europhys. Lett.* **27**, 421 (1994); P. Reimann (unpublished).
- [8] F. Marchesoni, *Phys. Lett. A* **237**, 26 (1998); P. S. Landa, *Phys. Rev. E* **58**, 1325 (1998); Ya. M. Blanter and M. Büttiker, *Phys. Rev. Lett.* **81**, 4040 (1998).
- [9] C. W. Gardiner, *Handbook of Stochastic Methods for Physics, Chemistry and the Natural Sciences* (Springer-Verlag, Berlin, 1983); H. Risken, *The Fokker-Planck Equation* (Springer-Verlag, Berlin, 1984); N. G. Van Kampen, *Stochastic Processes in Physics and Chemistry* (North-Holland, Amsterdam, 1992).
- [10] L. Ramírez-Piscina, J. M. Sancho, and A. Hernández-Machado, *Phys. Rev. B* **48**, 125 (1993); R. L. Honeycutt, *Phys. Rev. A* **45**, 600 (1992).